ChemPubSoc Europe
DOI: 10.1002/chem.201402623
CHEMISTRY
A European Journal
Full Paper

Dyads and Triads

Mono- and Bis(pyrrolo)tetrathiafulvalene Derivatives Tethered to C_{60}: Synthesis, Photophysical Studies, and Self-Assembled Monolayers

Marta Vico Solano,[a, b] Eduardo Antonio Della Pia,[b] Martyn Jevric,[b] Christina Schubert,[c] Xintai Wang,[b] Cornelia van der Pol,[a] Anders Kadziola,[b] Kasper Nørgaard,[b] Dirk M. Guldi,*[c] Mogens Brøndsted Nielsen,*[b] and Jan O. Jeppesen*[a]

Dedicated to Emeritus Professor Jan Becher on the occasion of his 75th birthday

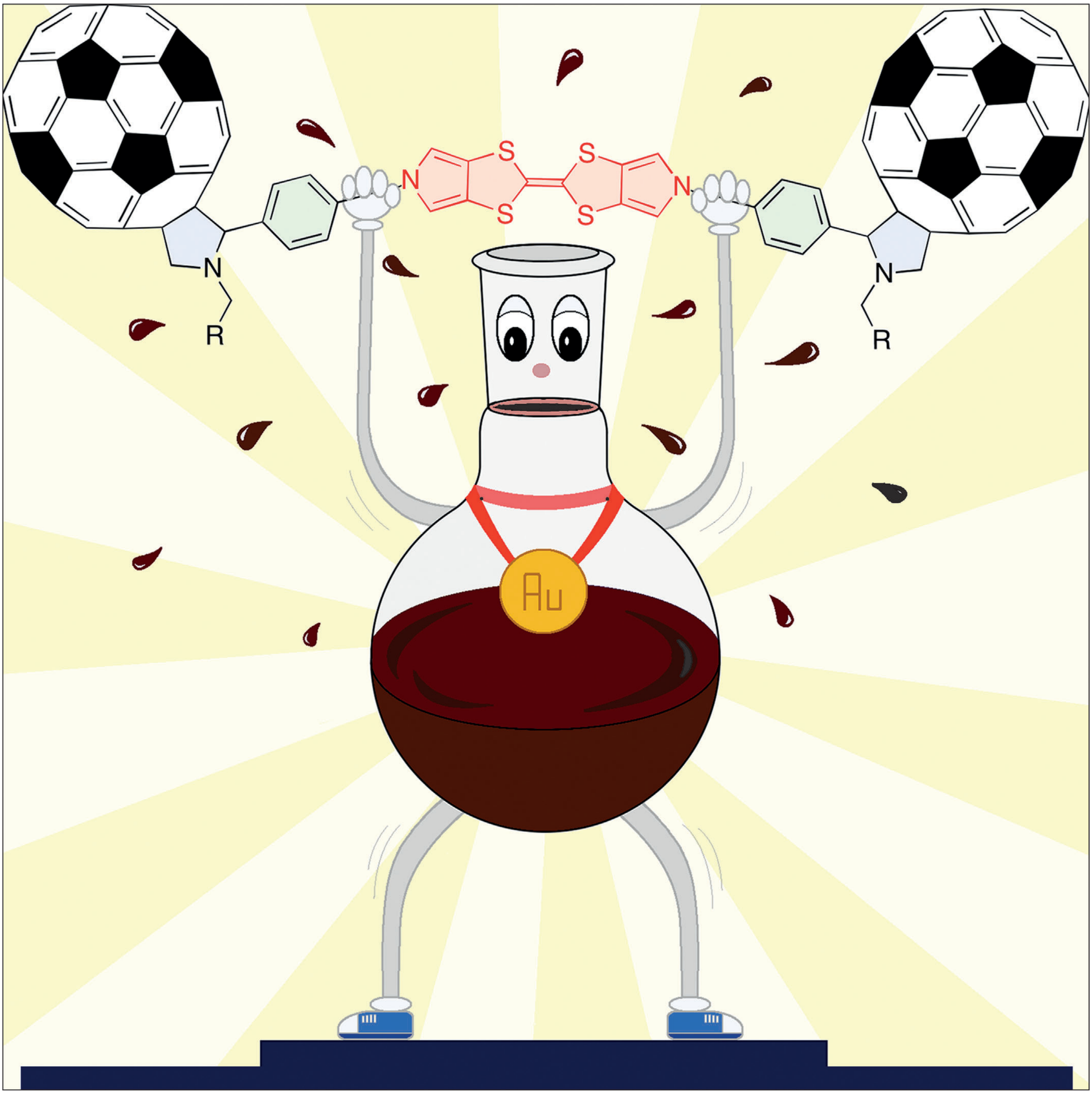

Abstract: A series of mono- (MPTTF) and bis(pyrrolo)tetrathiafulvalene (BPTTF) derivatives tethered to one or two C_{60} moieties was synthesized and characterized. The synthetic strategy for these dumbbell-shaped compounds was based on a 1,3-dipolar cycloaddition reaction between aldehyde-functionalized MPTTF/BPTTF derivatives, two different tailor-made amino acids, and C_{60}. Electronic communication between the MPTTF/BPTTF units and the C_{60} moieties was studied by a variety of techniques including cyclic voltammetry and absorption spectroscopy. These solution-based studies indicated no observable electronic communication between the MPTTF/BPTTF units and the C_{60} moieties. In addition, femtosecond and nanosecond transient absorption spectroscopy revealed, rather surprisingly, that no charge transfer from the MPTTF/BPTTF units to the C_{60} moieties takes place on excitation of the fullerene moiety. Finally, it was shown that the MPTTF–C_{60} and C_{60}–BPTTF-C_{60} dyad and triad molecules formed self-assembled monolayers on a Au(111) surface by anchoring to C_{60}.

Introduction

Tetrathiafulvalene (TTF, **1**, Figure 1) is a redox-active compound that can exist in three redox states (TTF^0, TTF^{+}, TTF^{2+}). Owing to these properties, TTF and its π-extended derivatives are particularly interesting as redox-active units in molecular electronics devices, with the possibility to switch between conducting ON–OFF states by applying, for example, a high bias potential or an external gating potential.[1] However, with their four peripheral positions, one drawback of functionalized TTFs is the existence of *cis/trans* isomers. This problem is avoided in the related bis(pyrrolo)tetrathiafulvalene (BPTTF, **2**), which has two NH groups available for further functionalization and exhibits the same reversible redox behavior as TTF.

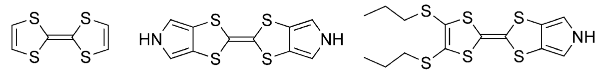

1 **2** **3**

Figure 1. Molecular structures of tetrathiafulvalene (TTF, **1**), bis(pyrrolo)tetrathiafulvalene (BPTTF, **2**), and monopyrrolotetrathiafulvalene (MPTTF, **3**) endowed with propylthio end groups.

For the construction of molecular junctions, suitable electrode anchoring groups are a crucial requirement. So far, the thiol group has been the most widely used anchoring group because of the strong S–Au bond.[2] Recently, Buckminsterfullerene (C_{60}), among others, has appeared as an alternative anchoring group[3] because of its capability to interact with gold electrodes through π overlap, which allows a better-defined contact region to the gold surface. Thus, dumbbell molecules with central phenylenediamine or fluorene units have been prepared by Prato reactions[4] and studied in different junctions.[3,5] For this reason, we became interested in exploring C_{60}–BPTTF–C_{60} electron-donor–acceptor triads, with three major objectives: 1) to develop efficient synthetic protocols, 2) to shed light on their photophysical properties, in particular in the context of elucidating whether any communication between the units exists, and 3) to investigate the possibility of forming self-assembled monolayers on gold as predecessors to their incorporation into molecular electronics devices.

A rigid C_{60}–TTF–C_{60} electron-donor–acceptor triad was previously prepared by a Diels–Alder reaction between tetramethylidene TTF and C_{60}.[6] However, the product suffered from poor solubility, and the C_{60} moieties had to be replaced by more soluble methanofullerene derivatives incorporating polyether groups to allow for detailed photophysical studies.[6] Significant interactions between the C_{60} and TTF units were observed in the ground state, and nanosecond transient absorption fluorescence spectroscopy revealed the formation of a charge-separated radical pair C_{60}–$TTF^{\bullet+}$–$C_{60}^{\bullet-}$. A charge-separated radical pair was also observed for a different kind of C_{60}–TTF–C_{60} electron-donor–acceptor triad, in which the C_{60} moieties were attached to the same end of the TTF unit.[7] Photolytic generation of radical pairs has also been observed in several electron-donor–acceptor dyads containing C_{60} and extended TTFs.[8,9] To the best of our knowledge, the effect of fusing the TTF unit to pyrrole in such electron-donor–acceptor conjugates has not been investigated.

The discovery of a reproducible large-scale synthesis of BPTTF (**2**) and monopyrrolotetrathiafulvalene (MPTTF, **3**, Figure 1) building blocks in the late 1990s[10,11] opened the door to incorporate redox-active MPTTF and BPTTF units into more elaborate structures, including macrocyclic and supra-

---

[a] Dr. M. V. Solano, Dr. C. van der Pol, Prof. Dr. J. O. Jeppesen
Department of Physics, Chemistry, and Pharmacy
University of Southern Denmark
Campusvej 55, 5230, Odense M (Denmark)
Fax: (+45) 6615-8780
E-mail: joj@sdu.dk

[b] Dr. M. V. Solano, Dr. E. A. Della Pia, Dr. M. Jevric, X. Wang,
Prof. Dr. A. Kadziola, Prof. Dr. K. Nørgaard, Prof. Dr. M. B. Nielsen
Department of Chemistry &
Center for Exploitation of Solar Energy & Nano-Science Center
University of Copenhagen
Universitetsparken 5, 2100 Copenhagen Ø (Denmark)
Fax: (+45) 3532-0212
E-mail: mbn@kiku.dk

[c] C. Schubert, Prof. Dr. D. M. Guldi
Department of Chemistry and Pharmacy and
Interdisciplinary Center for Molecular Materials
Lehrstuhl für Physikalische Chemie I
Friedrich-Alexander-Universität Erlangen-Nürnberg
Egerlandstrasse 3, 91058 Erlangen (Germany)
Fax: (+49) 9131-8528309
E-mail: guldi@chemie.uni-erlangen.de

Supporting information for this article is available on the WWW under http://dx.doi.org/10.1002/chem.201402623.

molecular systems. With the availability of these building blocks, we reasoned that it should be possible to functionalize the BPTTF unit through the pyrrole nitrogen atoms with C_{60} moieties to create fullerene dumbbells bridged by the BPTTF unit. To ensure close proximity between the electroactive units, we chose to separate them by only a single phenylene group as spacer.

Herein, we describe the synthesis and characterization of four fullerene dumbbells/half-dumbbells incorporating BPTTF or MPTTF units. They were synthesized by means of a modified Buchwald–Hartwig reaction followed by a [3+2] Prato cycloaddition reaction. The MPTTF/BPTTF–C_{60} conjugates were studied in detail by electrochemistry (both in solution and as self-assembled monolayers on gold) and UV/Vis absorption, fluorescence, and femtosecond pump–probe spectroscopy.

Results and Discussion

Synthesis

To chemically attach BPTTF and MPTTF units to C_{60}, we employed a synthetic strategy based on the Prato reaction.[4] On account of the typical solubility problems encountered in fullerene chemistry, more specifically related to the formation of C_{60} dumbbell structures, two tailor-made amino acids **4**[12] and **5** (Figure 2) were prepared, both of which contain solubilizing alkyl chains.

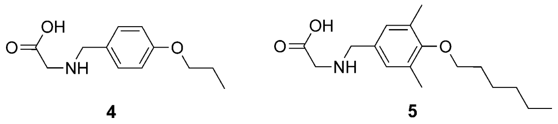

Figure 2. Molecular structures of amino acids **4** and **5**.

Amino acid **4** has previously been incorporated into fullerene–dihydroazulene photoswitches,[12b] which exhibited excellent solubilities in common organic solvents. The related amino acid **5** was synthesized in a similar manner to **4**. The synthesis of **5** initially involved transformation of the hydroxyl group in 4-bromo-2,6-xylenol (**6**) into the corresponding hexyl ether **7**,[13] mediated by the treatment of the phenol with hexyl iodide in the presence of potassium carbonate in refluxing acetone (Scheme 1). Subsequently, lithium–halogen exchange at −78 °C followed by treatment of the reaction mixture with anhydrous DMF resulted in the formylated derivative **8**. Finally, reductive amination followed by saponification and acidification of the reaction mixture to pH 6.7 gave **5** as a fluffy white solid.

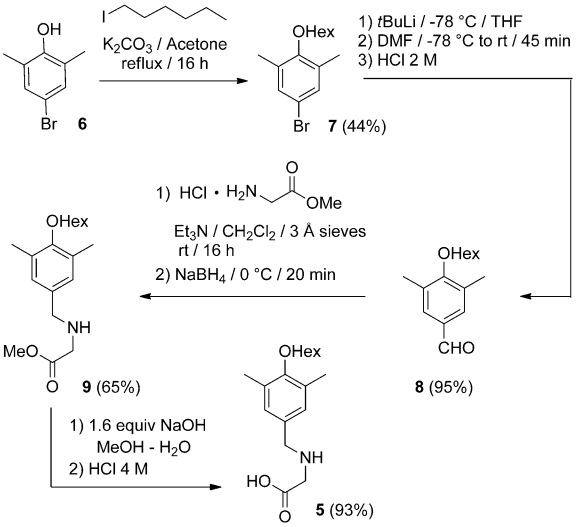

Scheme 1. Synthetic sequence for amino acid **5**.

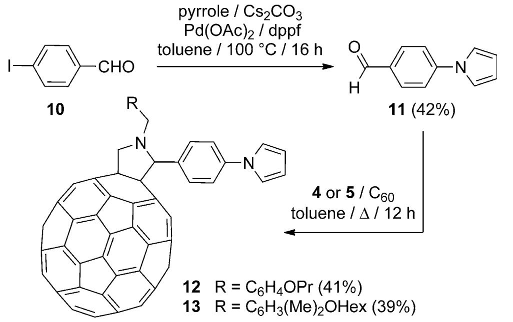

Scheme 2. Synthesis of C_{60}-end-capped phenylpyrrole derivatives **12** and **13** by the Prato reaction.

With amino acids **4** and **5** in hand, we investigated the scope of the Prato reaction with pyrrole-functionalized benzaldehyde derivatives, by first turning our attention (Scheme 2) to the model system 1-(4′-formylbenzyl)pyrrole (**11**). This compound, which does not contain the TTF redox unit, could be prepared in moderate yield (42 %) from 4-iodobenzaldehyde (**10**) in a typical Buchwald–Hartwig reaction[14] with $Pd(OAc)_2$ and bis(diphenylphosphino)ferrocene (dppf) as catalyst system. Thereafter, the ability of **11** to undergo conversion to an azomethine ylide and to participate in subsequent [3+2] cycloaddition with C_{60} was investigated by subjecting it to Prato reaction conditions in the presence of amino acids **4** and **5**. This resulted in formation of fulleropyrrolidines **12** and **13** in yields of 41 and 39 %, respectively. These products were isolated by using standard column chromatographic techniques and completely characterized.

We then focused on constructing a MPTTF derivative bearing carboxaldehyde functionality as a suitable precursor for the Prato reaction. An initial attempt to couple **3** and **10** under the conditions described above resulted in decomposition of the starting material. However, changing the catalytic metal from palladium to copper proved to be successful. Thus, by using an excess of CuI and *trans*-1,2-diaminocyclohexane, the desired product **14** was obtained in high yield (Scheme 3). Similar conditions were previously used for *N*-aryl amination of other MPTTFs.[15] The structure of **14** was confirmed by standard analytical techniques and X-ray crystallographic analysis (see Supporting Information). Then, **14** was subjected to standard Prato reaction conditions with amino acids **4** and **5** in refluxing toluene to give the two new fullerene derivatives **15**

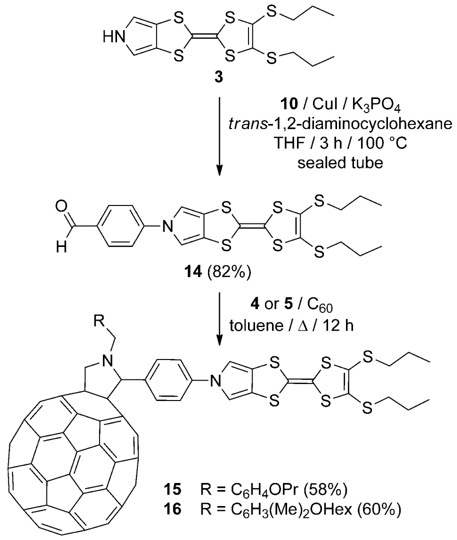

Scheme 3. Synthesis of C_{60}-end-capped MPTTF derivatives **15** and **16** using the Prato reaction.

and **16** bearing a redox-active MPTTF unit, again both in good yields. The ^{1}H NMR spectra for each derivative exhibited characteristic resonances at $\delta \approx 4.8$ and 4.0 ppm ($^2J = 9.5$ Hz) for the methylene protons of the pyrrolidine motif and an AB system resonating around $\delta = 4.4$ and 3.4 ppm ($^2J = 13$ Hz) for the diastereotopic benzylic protons of the solubilizing group. Evidence for the presence of the MPTTF unit was provided by the appearance of a 2H singlet at about $\delta = 6.4$ ppm for the α protons of the pyrrole moiety of the MPTTF unit. MALDI-TOF mass spectra showed the molecular ion for both products, and the observed isotope patterns were in agreement with the theoretically calculated ones.

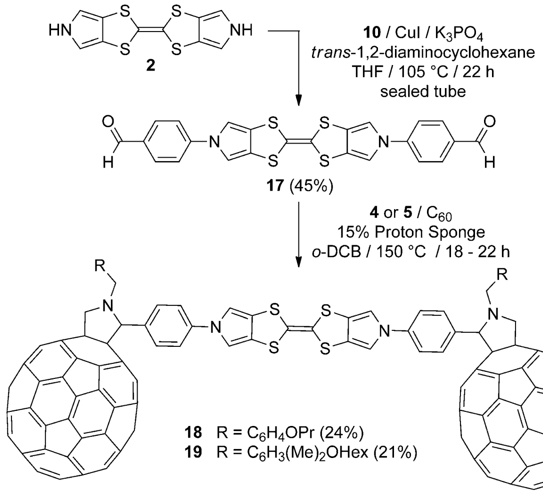

Scheme 4. Synthesis of the dumbbells **18** and **19** under modified Prato reaction conditions.

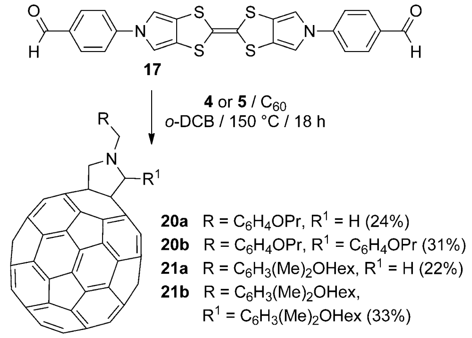

Scheme 5. Formation of byproducts **20a**–**b** and **21a**–**b**.

Our next objective was to prepare dumbbell-shaped C_{60}–BPTTF–C_{60} triads. Precursor dialdehyde **17** was synthesized by a CuI-catalyzed reaction between **2** and **10** (Scheme 4). The product was isolated as an orange solid, which was insoluble in standard organic solvents. Consequently, purification was limited to washing the precipitate with a broad spectrum of solvents ranging from water to *n*-pentane, which ultimately provided a pure sample of **17**. IR spectroscopic analysis of **17** revealed the presence of the carbonyl group by the stretching band observed at 1687 cm^{-1} and the absence of the NH stretching band observed around 3140 cm^{-1} for the starting material **2**. Of all solvents investigated, *o*-dichlorobenzene (*o*-DCB) proved best for solubilizing **2** and was chosen for the subsequent Prato reactions. However, our initial attempts only gave trace amounts of the desired dumbbell products **18** and **19** when a mixture of **17**, C_{60}, and an excess of amino acid **4** or **5** was heated to 150 °C for almost 1 d in *o*-DCB. Instead, products **20**–**21a** (22–24%) and **20**–**21b** (31–33%) were formed under these harsh reaction conditions (Scheme 5).[16] The BPTTF unit is susceptible to protonation,[11a] and the combination of a proton source in the form of the amino acid and application of excessive thermal energy to the system likely caused degradation of **17** and may somehow have facilitated the formation of formaldehyde and conversion of the amino acid to the corresponding aldehyde or iminium species, which could then undergo subsequent 1,3-dipolar cycloaddition to provide the suggested products. Indeed, the identities of **20**–**21a** and **20**–**21b** were confirmed by preparing them in a conventional manner from suitable starting materials (see Supporting Information). To avoid this undesired outcome, we carried out the Prato reactions in the presence of the non-nucleophilic base 1,8-bis(dimethylamino)naphthalene[17] (Proton Sponge, 15 mol%). Under these conditions, it was possible to isolate dumbbells **18** and **19** in yields of 24 and 21%, respectively. With regard to reproducibility, we note that the reactions did not always proceed successfully under these modified Prato conditions.[18] Owing to the very limited solubility of dialdehyde **17**, which restricted its purification, it is possible that some traces of copper salts could sometimes be present as impurities after the washing procedure mentioned above, and in such cases cause retro-cycloadditions, as reported by Martín and co-workers.[19] Products **18** and **19** were purified by standard column chromatography with CS_2 as cosolvent. Despite the presence of alkyl solubilizing chains, they exhibited limited solubility (in particular **18**), but it was possible to achieve full characterization. The ^{1}H NMR spectra of **18** and **19** exhibited the typical set of doublets at $\delta = 4.7$ and 4.0 ppm ($^2J = 9.5$ Hz), indicative of the methylene protons of the pyrrolidine ring. The presence of a 4H singlet at $\delta = 6.5$ ppm represented the solitary resonance of the BPTTF pyrrole protons outside the aromatic region. Despite the presence of two chiral centers in these dumbbells, only one set of signals was observed in the ^{1}H and ^{13}C NMR spectra. This observation can most likely be accounted for by the fact that the two chiral centers are remote from one another. MALDI-TOF mass spectrometry gave molecular ions for each dumbbell and also provided isotopic patterns in agreement with calculations.

Electrochemistry

Cyclic voltammetry (CV) was carried out on the majority of the new redox-active compounds in THF or CH_2Cl_2 with 0.1 M nBu$_4$NPF$_6$ as supporting electrolyte. The data are summarized in Table 1, and Figure 3 shows the cyclic voltammograms of **3**, **13**, and **15** (additional CVs can be found in the Supporting Information). All MPTTF derivatives exhibit two reversible one-electron oxidations that correspond to the formation of the TTF radical cation and dication. The oxidation potentials for the MPTTF unit did not change significantly by tethering of C_{60}, as seen by comparing the oxidation potentials of **15** and **16** to those of **3**. Likewise, the fullerene electrochemistry, that is, addition of up to three electrons, was itself unaltered by the presence of the MPTTF unit, as seen by comparing the reduction potentials of **12** and **13** with those of **15** and **16**, respectively. Electrochemical data for dumbbells **18** and **19** were acquired by differential pulse voltammetry (DPV) in o-DCB containing 0.1 M nBu$_4$NPF$_6$ (Table 1); this solvent was chosen on account of the very low solubility of these compounds in dichloromethane. Both dumbbells **18** and **19** exhibited two one-electron oxidations accompanied by a two-electron reduction at −0.99 V for the simultaneous reduction of both fullerenes. Moreover, from the difference between the first oxidation and first reduction processes, we could estimate a HOMO–LUMO gap of approximately 1.15 eV. Thus, electron transfer from the fullerene singlet excited state with an energy of 1.76 eV seems feasible to afford a charge separated state (see below).

Table 1. Electrochemical data (potentials vs. Fc$^+$/Fc) of the C_{60} end-capped derivatives **12**, **13**, **15**, **16** and corresponding reference compounds **2** and **3**, determined by CV,[a,b] and of dumbbells **18** and **19**, determined by DPV.[c]

Compound	E^2_{ox} [V]	E^1_{ox} [V]	E^1_{red} [V]	E^2_{red} [V]	E^3_{red} [V]
2[a]	+0.28	+0.03	–	–	–
3[b]	+0.38	+0.03	–	–	–
12[b]	–	–	−1.10	−1.49	−2.02
13[b]	–	–	−1.12	−1.49	−2.04
15[b]	+0.40	+0.03	−1.12	−1.49	−2.03
16[b]	+0.41	+0.03	−1.14	−1.51	−2.03
18[c]	+0.54	+0.15	−0.99	–	–
19[c]	+0.55	+0.16	−0.99	–	–

[a] THF + 0.1 M nBu$_4$NPF$_6$; scan rate 0.1 V s^{-1}. [b] CH_2Cl_2 + 0.1 M nBu$_4$NPF$_6$; scan rate 0.1 V s^{-1}. [c] o-DCB + 0.1 M nBu$_4$NPF$_6$. Temperature 295 K. Working electrode: glassy carbon; counter electrode: platinum; reference electrode: Ag/Ag$^+$.

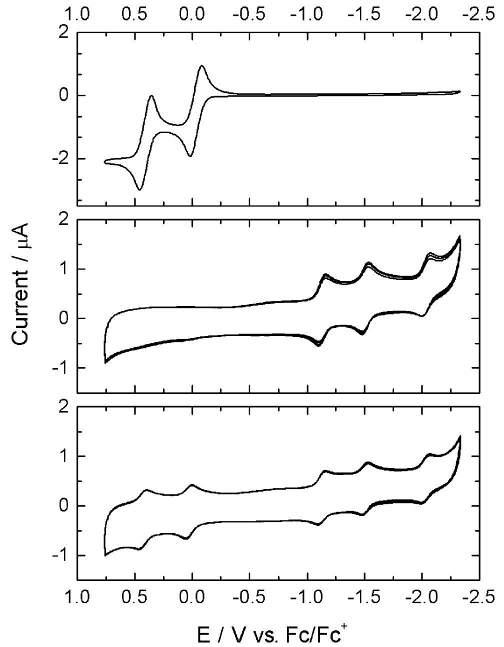

Figure 3. CVs of **3** (top), C_{60} derivative **13** (middle), and MPTTF–C_{60} dyad **15** (bottom) recorded in CH_2Cl_2 containing nBu$_4$NPF$_6$ (0.1 M). Potentials versus Fc$^+$/Fc.

UV/Vis spectroscopy

The optical absorption features of the dumbbells and the other C_{60}-end-capped derivatives together with suitable reference compounds were recorded in o-DCB, and the obtained data are collected in Table 2. The absorption spectra of **3**, **13**, **16**, and **18** in o-DCB are shown in Figure 4. The absorption spectra of electron-donor–acceptor triads **18** and **19** show su-

Table 2. Photophysical data for compounds **3**, **12**, **13**, **15**, **16**, **18**, and **19** recorded in o-DCB at room temperature.

Compound	λ_{abs} [nm]	λ_{em} [nm]	ϕ_f [10^{-4}][a]
3	329, 458 (sh)	n.a.	n.a.
12	327 (sh), 433, 475 (sh), 546 (sh), 613 (sh) 637 (sh), 704	712, 791	7.6
13	327 (sh), 433, 475 (sh), 546 (sh), 613 (sh) 637 (sh), 704	712, 791	7.1
15	332, 433, 475 (sh), 546 (sh), 613 (sh) 637 (sh), 704	713, 790 (sh)	1.6
16	332, 433, 475 (sh), 546 (sh), 613 (sh) 637 (sh), 704	713, 790 (sh)	1.1
18	330, 432, 475 (sh), 546 (sh), 613 (sh) 637 (sh), 704	712, 789	1.6
19	327 (sh), 432, 475 (sh), 546 (sh), 613 (sh) 637 (sh), 704	712, 791	2.6

[a] Quantum yields were determined with C_{60} as reference ($\phi_f = 3.0 \times 10^{-4}$ in o-DCB[20]).

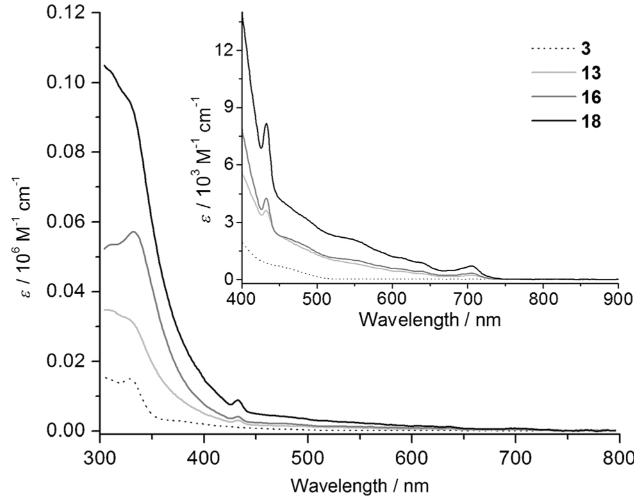

Figure 4. Absorption spectra of compounds **13**, **16**, and **18** in *o*-DCB. The spectrum of **3** (dotted line) is included for comparison. The inset shows an enlargement of the 400–900 nm region.

perimposed features of the fulleropyrrolidines **12** and **13** together with those of BPTTF (**2**). This indicates that both electroactive units (i.e., BPTTF and C_{60}) preserve their identity in the corresponding C_{60}–BPTTF–C_{60} triads **18** and **19** with no significant electronic interaction in the ground state. The absorption spectra of the electron-donor–acceptor dyads and triads reveal the C_{60}-centered band around 430 nm as well as the fundamentally important 0–0 transition at about 700 nm, which originates from the monofunctionalization of C_{60} and reflects the partially broken symmetry (C_s) relative to pristine C_{60} (I_h). To investigate the possibility of charge transfer (CT) between the C_{60} and the BPTTF moieties, the absorption properties were studied in a variety of solvents (CS_2, acetonitrile, benzonitrile, THF). However, no CT band was observed for the two dumbbells and a good agreement between the UV/Vis spectra of the dumbbells and the sum of those of their molecular constituents was established in the different solvents.

Fluorescence spectroscopy

Investigations into excited-state interactions were based on steady-state fluorescence measurements (Table 2). An example of emission and excitation spectra is shown in Figure 5 for compound **15**. Compound **15** shows a fluorescence maximum at 713 nm, followed by a shoulder at 790 nm that was not observed in the emission spectrum of **3**, which only showed a broad peak centered at about 440 nm, and a fluorescence quantum yield of 1.6×10^{-4} ($\pm$10%) in *o*-DCB. Fluorescence quantum yields were determined by exciting the electron-acceptor moiety at 470 nm and using C_{60} as reference ($\phi_f = 3.0\times10^{-4}$ in *o*-DCB[20]). In the dumbbells, the main emission feature is seen at 712 nm. The fluorescence quantum yields of MPTTF–C_{60} and C_{60}–BPTTF–C_{60} compounds **15**–**19** are lower than those of compounds **12** and **13**, which do not contain a TTF unit, but the quenching effect exerted by the MPTTF and BPTTF units seems quite small.

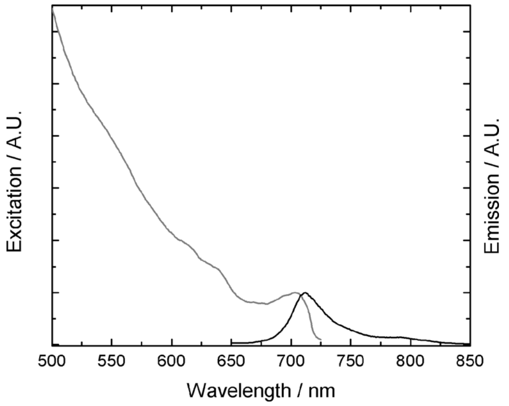

Figure 5. Normalized excitation (gray line) and emission (black line) of **15** in *o*-DCB at 298 K.

Femtosecond transient absorption spectroscopy

To shed further light on the properties of the excited state, femtosecond transient absorption measurements on C_{60}–BPTTF–C_{60} electron-donor–acceptor triads **18** and **19** and their reference compounds were carried out in anisole and benzonitrile. All of the systems were probed with 150 fs laser pulses. Excitation of the pyrrolidino–C_{60} unit at 387 nm populates its singlet excited state, which exhibits characteristic absorption maxima at 504 and 918 nm (Figure 6). The singlet excited state undergoes intersystem crossing (ISC) to the corresponding triplet manifold with characteristic lifetimes of 1.4 ns. Evidence for the latter comes from a differential absorption spectrum that shows a 700 nm maximum. MPTTF–C_{60} derivatives **15** and **16** together with **18** and **19** showed similar features. The singlet decay dynamics were analyzed by following the absorption decay at 918 nm, and the growth of the triplet was analyzed by following the absorption at 700 nm (Figure 7). Fitting of these time absorption profiles gave rate constants for ISC of 8.3×10^{8}. This is in sound agreement with the only weakly quenched C_{60}-centered fluorescence.

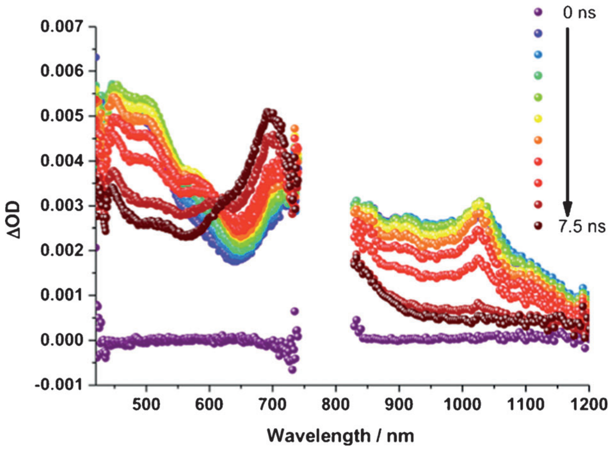

Figure 6. Differential absorption spectra (Vis and NIR) obtained by femtosecond flash photolysis (387 nm, 200 nJ) of **19** in argon-saturated benzonitrile with several time delays between 0 and 7500 ps.

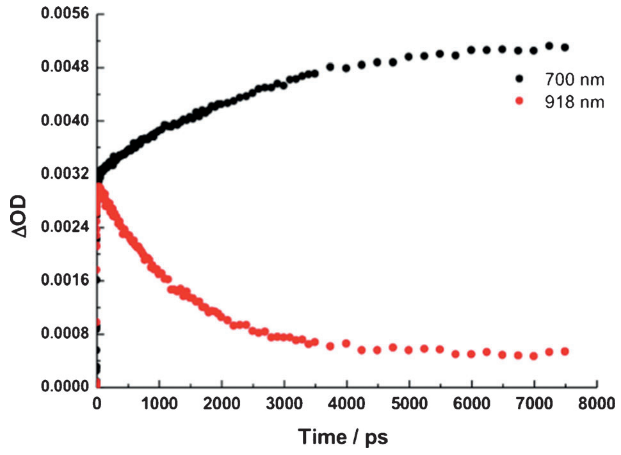

Figure 7. Absorption–time profiles at 700 and 918 nm monitoring the decay of the singlet excited state and the growth of the triplet excited state.

In nanosecond flash photolysis experiments, the triplet excited state of **19** was probed in argon-saturated anisole and benzonitrile. The lifetime of the triplet excited state was about 10 μs in both solvents. Moreover, the triplet quantum yield was nearly the same in both solvents. In the presence of molecular oxygen, the triplet excited state experiences a concentration-dependent deactivation process to form singlet oxygen quantitatively. More precisely, singlet-oxygen quantum yields suggested that the triplet was formed with quantum yields of 0.61 and 0.62 in anisole and benzonitrile, respectively.

All of these results suggest that intersystem crossing converting the fullerene singlet excited state (1.76 eV) to the corresponding triplet excited state (1.53 eV) is the favored deactivation process after excitation of these dumbbells, whereas formation of a charge-separated state (1.15 eV) is, at best, a minor component.

Self-assembled monolayers on gold

Several self-assembled monolayers (SAMs) of TTF derivatives on gold have been reported, but usually with TTFs terminated by an alkanethiol group.[21] SAMs of selected compounds were grown on single-crystal Au(111) substrates by immersion (48 h) in 50 μм toluene solutions of the respective compound. The quality of the grown SAMs was characterized by CV with the covered Au(111) substrate as working electrode. Figure 8 shows CV responses of $K_3[Fe(CN)_6]$ with SAM-modified gold electrodes containing the MPTTF derivative **3**, MPTTF–C_{60} dyad **16**, and the C_{60}–BPTTF–C_{60} dumbbell **19**. The peaks for the Fe^{2+}/Fe^{3+} redox signals nearly vanish (ratio between the integrated current peaks $I_{C60MPTTF}/I_{Au} = 0.063$) when SAMs of MPTTF–$C_{60}$ **16** cover the Au electrode, which implies that the molecules form high-density monolayers that block access to the Au surface. Similarly, C_{60}–BPTTF–C_{60} triad **19** formed monolayers on the Au electrode, albeit with slightly lower surface coverage ($I_{dumbbell}/I_{Au} = 0.33$). The MPTTF derivative **3** does not form particularly dense monolayers on Au(111) under similar experimental conditions.

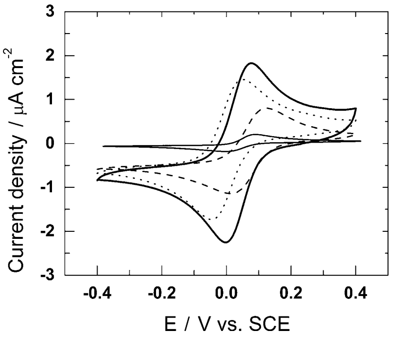

Figure 8. CVs of $K_3[Fe(CN)_6]$ for SAMs of MPTTF **3** (dotted line), MPTTF–C_{60} **16** (thin solid line), and C_{60}–BPTTF–C_{60} **19** (dashed line) on a single-crystal Au(111) electrode. The thick solid line is the CV response of the bare gold electrode. The voltammograms were recorded in argon-saturated aqueous solutions of 10 mм $K_3[Fe(CN)_6]$ with 0.1 м KCl. The scan rate was 50 mV s^{-1}.

The surface electrochemical responses of SAMs of MPTTF–C_{60} dyad **16** and C_{60}–BPTTF–C_{60} triad **19** were further recorded in dichloromethane with 1 mм nBu$_4$NClO$_4$ as electrolyte (Figure 9). The two one-electron oxidation events for the MPTTF units were observed for the SAMs at around $E = +0.5$ and $+0.78$ V (**16**) and $+0.35$ and $+0.74$ V (**19**) versus SCE.

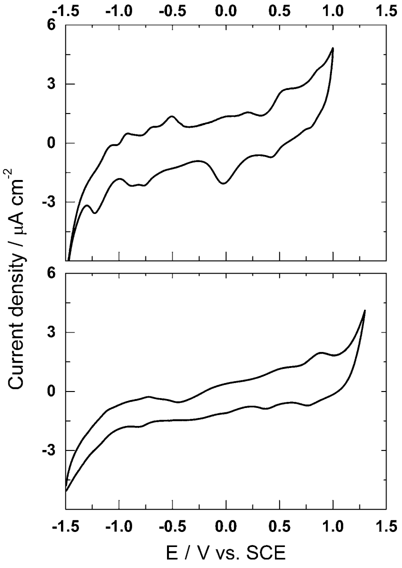

Figure 9. Electrochemical response from SAMs of **16** (top) and dumbbell **19** (bottom) on an Au(111) electrode. The voltammograms were recorded in solutions of 1 mм nBu$_4$ClO$_4$ in dichloromethane with a scan rate of 100 mV s^{-1}.

Also, the peaks corresponding to the C_{60} reductions could be observed in the range -1.3 to -0.5 V versus SCE for both types of SAMs. Sequential scans in the positive and negative directions (Supporting Information) confirm these observations. In the full CV, an additional peak was observed in SAMs of MPTTF–C_{60} **16**, centered around $E = 0$ V versus SCE. This peak may arise from desorption of molecules from the electrodes. The similarity between the recorded surface electrochemistry for SAMs of **16** and **19** indicates that, for both compounds, the fullerene moieties act as anchoring groups that contacts the electrode. For the C_{60}–BPTTF–C_{60} dumbbell **19** this orientation would result in the molecule lying flat on the surface, which is consistent with the less dense packing of these SAMs compared to SAMs of MPTTF–C_{60}, in which only a single C_{60} unit is attached to the electrode. A possible binding motif of MPTTF–C_{60} SAMs through the thioether sulfur atoms is unlikely to be prevalent and, to the best of our knowledge, there are no reported literature examples of SAMs formed from TTF-SR (R = alkyl) derivatives (and MPTTF **3** did not form particularly dense monolayers), whereas SAMs of TTF dithiolates have been fabricated.[22]

Conclusion

A versatile protocol for the synthesis of MPTTF and BPTTF molecules tethered to C_{60} was successfully developed by using tailor-made amino acid substrates. The 1,3-dipolar cycloaddition reactions to form C_{60}–BPTTF–C_{60} electron-donor–acceptor dumbbells **18** and **19** were complicated by competitive side reactions forming rather unexpected byproducts, but using Proton Sponge as an additive provided improved conditions, and these triads were consequently isolated in 21–24 % yields.

Detailed physicochemical studies reveal that the C_{60} and BPTTF units do not interact. With respect to the ground state, neither absorption spectroscopy nor electrochemistry point to any appreciable differences between **18** and **19**, on the one hand, and the corresponding reference compounds, on the other. With respect to the excited state, we conclude from steady-state and time-resolved measurements by means of fluorescence and pump–probe techniques that **18**, **19**, and the corresponding references are deactivated in a similar way. In short, intersystem crossing from the C_{60} singlet excited state to the corresponding triplet manifold is the predominant deactivation process after excitation. Competition with electron-transfer-induced deactivation cannot be ruled out on thermodynamic grounds. Experiments, however, lead us to suggest that electron transfer is at best a minor and inefficient process. This observation is rather surprising, as it contradicts recent investigations on other TTF–C_{60} electron-donor–acceptor conjugates.

Finally, the dumbbell-shaped electron-acceptor–donor–acceptor triad C_{60}–BPTTF–C_{60} **19** forms self-assembled monolayers on gold in which both C_{60} units seem to be in contact with gold, that is, the molecules lie flat on the surface. The electron-donor–acceptor dyad MPTTF–C_{60} **16** forms more densely packed monolayers that seem to be anchored to the surface primarily via the single fullerene unit. This arrangement is convenient for future incorporation of such monolayers in molecular electronics devices.

Experimental Section

General

All reagents were obtained from commercial suppliers and used without further purification unless otherwise indicated. Anhydrous solvents were obtained from a Solvent Purification System (Innovative Technology, Inc.). Anhydrous THF was distilled from the sodium–benzophenone couple. All reactions were performed under an inert atmosphere of argon if not otherwise stated. All reactions involving C_{60} were carried out in the absence of light. Purification of products was carried out by flash chromatography on silica gel (ROCC 40–63 μm). TLC was carried out on aluminum sheets precoated with silica gel 60F (Merck F_{254}). ^{1}H NMR (500 MHz) and ^{13}C NMR APT (125 MHz) spectra were recorded at 298 K on an instrument with non-inverse cryoprobe by using the residual solvent as the internal standard ($CDCl_3$: ^{1}H 7.26 ppm and ^{13}C 77.16 ppm, CD_3OD: ^{1}H 4.87 ppm and ^{13}C: 49.00 ppm, [D_6]DMSO: ^{1}H: 2.50 ppm and ^{13}C: 39.52 ppm, C_6D_6: ^{1}H: 7.16 ppm and ^{13}C: 128 ppm). All chemical shifts are quoted on the δ scale (ppm). In APT spectra (see Supporting Information), CH and CH_3 correspond to negative signals and C and CH_2 to positive signals. MALDI mass spectra were recorded on a time-of-flight apparatus by using *trans*-2-[3-(4-*tert*-butylphenyl)-2-methyl-2-propenylidene]malononitrile (DCTB) as matrix. IR spectra were obtained using the ATR Platinum Diamond 1 Refl accessory. Melting points were obtained with an automatic melting point apparatus SMP40 and are uncorrected. Elemental analyses were performed at London Metropolitan University or at the University of Copenhagen. Amino acid **4**,[12] BPTTF **2**,[10] and MPTTF **3**[11] were synthesized according to the respective literature procedures. Procedures for synthesis of **20 a**,**b** and **21 a**,**b** are described in the Supporting Information.

UV/Vis spectroscopy

UV/Vis absorption spectra were recorded at 298 K with a Lambda 2 UV/Vis spectrophotometer (PerkinElmer) in quartz cells of 1 cm path (concentration range 1–100 μM).

Steady-state fluorescence spectroscopy

A Horiba Jobin Yvon Fluoromax 3 spectrophotometer was used to perform fluorescence spectroscopy measurements at room temperature (298 K) in a 1 cm quartz cuvette. All spectra were corrected for the instrument response. For excitation wavelengths below 450 nm a cutoff filter (435 nm) was inserted.

Femtosecond transient absorption spectroscopy

Femtosecond transient absorption studies were performed with 387 nm laser pulses (1 kHz, 150 fs pulse width) from an amplified Ti/sapphire laser system (output 775 nm). For an excitation wavelength of 470 nm a nonlinear optical parametric converter was used to generate ultrashort tunable visible pulses from the pump pulses. The transient absorption pump–probe spectrometer is a two-beam setup in which the pump pulse is used as excitation source for transient species and the delay of the probe pulse is exactly controlled by an optical delay rail. As probe (white light continuum), a small fraction of pulses stemming from the laser system was focused by a 50 mm lens into a 2 mm-thick sapphire disc. The transient spectra were recorded on fresh oxygen-free solutions for each laser excitation. All experiments were performed at 298 K in a 2 mm quartz cuvette.

Nanosecond transient absorption spectroscopy

Nanosecond laser flash photolysis experiments were performed with 355 laser pulses from a Nd:YAG system (6 ns pulse width).

Electrochemical measurements in solution

Experiments were performed in a one-compartment glass electrochemical cell fitted with a Teflon cap. The working electrode consisted of a 5 mm-diameter platinum disk and the counter electrode was a platinum wire sealed in glass. The reference electrode was Ag/Ag$^+$, whereby the electrolyte solution was added to a glass tube containing a Ag wire separated from the solution by a porous tip. All potentials are referred to ferrocene/ferrocinium; ferrocene was also used as an internal standard to check for reference-electrode drift during the experiments. The measurements were performed at a scan rate of 0.1 V s^{-1} at 25 °C under an inert atmosphere and the solution was deaerated by nitrogen bubbling before the measurements. Nitrogen flowed on top of the solution during all the experiments. The compounds were first dissolved in CH_2Cl_2 or *o*-DCB to obtain a millimolar concentration. The solution was then mixed 50:50 with a solution of 0.2 M nBu$_4$NPF$_6$ in CH_2Cl_2 or *o*-DCB to give a final nBu$_4$NPF$_6$ concentration of 0.1 M.

Preparation of and electrochemical studies on SAMs

50 μM solutions of compounds were prepared by dissolution in toluene (Sigma-Aldrich, 99%). Commercial Au(111) disk (SPL, The Netherlands & MaTeck, Germany) with a diameter of approximately 8.7 mm as well as smaller homemade single-crystal Au(111) electrodes with diameters of approximately 1–2 mm were annealed at 900 °C for 8 h, followed by quenching in a hydrogen flame and rinsing with Millipore water. The quenching step was repeated several times. The quenched electrodes were immersed in the prepared solutions for 48 h. Cyclic voltammetry was carried out with an AutoLab Potentiostat 12 (Eco Chemie, The Netherlands) in a three-electrode electrochemical cell. Freshly prepared reversible hydrogen electrode (RHE) was used as the reference electrode for tests in aqueous solution (calibrated by SCE afterwards) and organic-phase SCE was used as reference electrode in organic solution. A Pt wire was used as the counter electrode. For aqueous-phase electrochemistry, 10 mM $K_3[Fe(CN)_6]$ (Sigma-Aldrich, 96%) in 0.1 M KCl was used as electrolyte, and for organic-phase electrochemistry, a 1 mM solution of nBu$_4$NClO$_4$ (Sigma-Aldrich, >98%) in dichloromethane (Sigma Aldrich, 98%) was used as electrolyte. High-purity argon gas (99.999%) was bubbled through the solutions for approximately 1 h to remove oxygen. The GPES program was employed to control electrochemical measurements. All glass equipment was boiled in 30% nitric acid and washed in deionized water before use.

Synthesis

1-Bromo-4-hexyloxy-3,5-dimethylbenzene (7): Prepared by using a modified literature procedure.[13] A mixture of 4-bromo-2,6-xylenol (6.00 g, 29.8 mmol), K_2CO_3 (5.43 g, 39.2 mmol), and 1-iodohexane (15.42 g, 72 mmol) in anhydrous acetone (250 mL) was heated under reflux for 16 h. The mixture was allowed to cool to RT and filtered. The filtrate was concentrated under reduced pressure to give a soapy crude material, which was subsequently purified by column chromatography (SiO_2, gradient elution with 5–20% toluene/heptane) to afford pure **7** (3.75 g, 44%) as a colorless oil. ^{1}H NMR (500 MHz, $CDCl_3$): $\delta = 7.13$ (s, 2H, ArH), 3.72 (t, $J = 6.6$ Hz, 2H, OCH_2), 2.24 (s, 6H, 2×$ArCH_3$), 1.81–1.75 (m, 2H, CH_2), 1.52–1.46 (m, 2H, CH_2), 1.36–1.33 (m, 4H, 2×CH_2), 0.92 ppm (t, $J = 6.9$ Hz, 3H, CH_2CH_3); ^{13}C NMR (125 MHz, $CDCl_3$): $\delta = 155.4$, 133.3, 131.5, 116.2, 72.6, 31.9, 30.5, 25.9, 22.8, 16.3, 14.2 ppm; MS (ESP +ve): *m/z* 286 $[M+H]^+$.

4-(Hexyloxy)-3,5-dimethylbenzaldehyde (8): *t*BuLi (1.7 M in pentane, 42 mL, 0.071 mol) was carefully added dropwise to a degassed solution of compound **7** (8.5 g, 29.8 mmol) in anhydrous THF (150 mL), at −78 °C. After the addition was complete, stirring was continued for a further 15 min at −78 °C, after which anhydrous DMF was added (10 mL, 0.13 mol), the cold bath removed, and the reaction vessel allowed to reach ambient temperature. The vessel was then cooled to 0 °C and the mixture acidified with aqueous 2 M HCl (100 mL). The aqueous phase was then extracted with Et_2O (3×100 mL). The combined organic phases were dried over $MgSO_4$, filtered, and the solvent evaporated under reduced pressure to give an oil that was purified by column chromatography (SiO_2, toluene), giving **8** (6.63 g, 95%) as a colorless oil. $R_f = 0.12$ (toluene); ^{1}H NMR (500 MHz, $CDCl_3$): $\delta = 9.87$ (s, 1H, CHO), 7.54 (s, 2H, ArH), 3.81 (t, $J = 6.6$ Hz, 2H, OCH_2), 2.33 (s, 6H, 2×$ArCH_3$), 1.85–1.79 (m, 2H, CH_2), 1.54–1.48 (m, 2H, CH_2), 1.38–1.34 (m, 4H, 2×CH_2), 0.92 ppm (t, $J = 7.1$ Hz, 3H, CH_2CH_3); ^{13}C NMR (125 MHz, $CDCl_3$): $\delta = 191.8$, 161.8, 132.2, 132.1, 130.8, 72.7, 31.8, 30.5, 25.9, 22.7, 16.5, 14.2 ppm; MS (ESP +ve): *m/z* 235 $[M+H]^+$; elemental analysis calcd (%) for $C_{15}H_{22}O_2$: C 76.88, H 9.46; found: C 76.67, H 9.32.

Methyl-2-[(4-(hexyloxy)-3,5-dimethylbenzyl)amino]acetate (9): 3 Å molecular sieves (ca. 10 g) were added to a mixture of aldehyde **8** (5.91 g, 40.1 mmol), glycine methyl ester hydrochloride (5.0 g, 39.8 mmol), and Et_3N (6.0 mL, 43 mmol) in anhydrous CH_2Cl_2 (90 mL) and the resulting mixture was stirred for 16 h. The reaction mixture was filtered and the solvent removed from the filtrate under reduced pressure. The resulting white solid was dissolved in MeOH (65 mL) and the solution cooled on an ice bath, and then sodium borohydride (1.57 g, 42.5 mmol) was added carefully to the stirred solution. After 10 min, aqueous saturated sodium bicarbonate (100 mL) was added to the reaction mixture. The phases were separated and the aqueous phase extracted with CH_2Cl_2 (3×100 mL). The combined organic phases were dried over Na_2SO_4, filtered, and the solvent evaporated in vacuo to give **9** as a pure colorless oil (8.02 g, 65%). $R_f = 0.35$ (ethyl acetate/heptane 3/2); ^{1}H NMR (500 MHz, $CDCl_3$): $\delta = 6.96$ (s, 2H, ArH), 3.74–3.71 (m, 5H, CH_2CH_2O and CO_2CH_3), 3.69 (s, 2H), 3.48 (s, 2H), 2.25 (s, 6H, 2×$ArCH_3$), 1.81–1.76 (m, 2H, CH_2), 1.52–1.46 (m, 2H, CH_2), 1.37–1.33 (m, 4H, 2×CH_2), 0.91 ppm (t, $J = 7.1$ Hz, 3H, CH_2CH_3), NH not observable; ^{13}C NMR (125 MHz, $CDCl_3$): $\delta = 172.8$, 155.5, 134.1, 131.1, 128.9, 72.5, 52.9, 51.9, 49.9, 31.9, 30.5, 26.0, 22.8, 16.4, 14.2 ppm; MS (ESP +ve): *m/z* 308 $[M+H]^+$; elemental analysis calcd (%) for $C_{18}H_{29}NO_3$: C 70.32, H 9.51, N 4.56; found: C 70.40, H 9.63, N 4.64.

2-{[4-(Hexyloxy)-3,5-dimethylbenzy]amino}acetic acid (5): NaOH (1.03 g, 41.7 mmol) was added to a stirred solution of compound **9** (5.53 g, 17.9 mmol) in 50% aqueous MeOH (100 mL) and the stirring continued until TLC (EtOAc/heptanes 3/2) indicated complete consumption of **9**. The solution was then concentrated to about 50 mL by rotary evaporation and diluted with H_2O (50 mL). To this stirred solution was added aqueous 4 M HCl until pH 6.7. The resulting white precipitate was collected by filtration and washed with H_2O (4×20 mL) to afford **5** (4.96 g, 93%) as a white fluffy solid. M.p. >181 °C (decomp); ^{1}H NMR (500 MHz, CD_3OD): $\delta = 7.13$ (s, 2H, ArH), 4.07 (s, 2H), 3.78 (t, $J = 6.4$ Hz, 2H, OCH_2), 3.45 (s, 2H), 2.28 (s, 6H, 2×$ArCH_3$), 1.83–1.77 (m, 2H, CH_2), 1.57–1.51 (m, 2H, CH_2), 1.40–1.37 (m, 4H, 2×CH_2), 0.94 ppm (t, $J = 7.1$ Hz, 3H, CH_2CH_3); ^{13}C NMR (125 MHz, CD_3OD): $\delta = 170.7$, 158.3, 133.1, 131.5, 127.9, 73.4, 51.5, 49.6, 32.9, 31.4, 26.9, 23.7, 16.4, 14.4 ppm; MS (ESP +ve): *m/z* 316.40 $[M+Na]^+$; elemental analysis calcd (%) for $C_{17}H_{27}NO_3$: C 69.59, H 9.28, N 4.77; found: C 69.67, H 9.19, N 4.85.

1-(4′-Formylphenyl)pyrrole (11): A degassed solution of pyrrole (0.20 mL, 2.88 mmol) in toluene (20 mL) was added by cannula to a microwave tube containing 4-iodobenzaldehyde (1.09 g, 4.70 mmol), $Pd(OAc)_2$ (31 mg, 0.140 mol), Cs_2CO_3 (984 mg, 3.02 mmol), and 1,1′-bis(diphenylphosphino)ferrocene (dppf) (79 mg, 0.142 mol). The vessel was heated conventionally for 16 h at 100 °C. The vessel was allowed to cool to RT and the crude reaction mixture passed through a pad of Celite and washed several times with CH_2Cl_2. The solvent was removed in vacuo and the crude residue subsequently purified by flash column chromatography (SiO_2, CH_2Cl_2) to furnish **11** (205 mg, 42 %) as an off-white solid. $R_f=0.25$ (CH_2Cl_2); m.p. 72.5–73.6 °C; ^1H NMR (500 MHz, $CDCl_3$): $\delta=10.00$ (s, 1 H, CHO), 7.95 (d, 2 H, $J=8.6$ Hz, ArH), 7.55 (d, 2 H, $J=8.6$ Hz, ArH), 7.19 (app. t, 2 H, $J=2.2$ Hz, pyrrole α-H), 6.41 ppm (app. t, 2 H, $J=2.2$ Hz, pyrrole β-H); ^{13}C NMR (125 MHz, $CDCl_3$): $\delta=191.0$, 145.2, 133.5, 131.7, 119.9, 119.2, 112.1 ppm; IR (ATR): $\tilde{\nu}=3129$, 3107, 2824, 2804, 2731, 1750, 1684, 1600, 1582, 1471, 1331, 1171, 1065, 824, 723 cm^{-1}; MS (ESP +ve): *m/z* 194 $[M+Na]^+$, 172 $[M+H]^+$; elemental analysis calcd (%) for $C_{11}H_9NO$: C 77.17, H 5.30, N 8.18; found: C 76.85, H 5.12, N 8.16.

Compound 12: A mixture consisting of C_{60} (141 mg, 0.196 mmol), **11** (20 mg, 0.117 mmol), and amino acid **4** (132 mg, 0.591 mmol) in degassed toluene (50 mL) was heated under reflux for 12 h. The reaction mixture was cooled to RT and the solvent evaporated under reduced pressure to give a brown residue, which was subjected to purification by flash chromatography (SiO_2, gradient elution with 1–10 % toluene/CS_2) to afford compound **12** (50 mg, 41 %) as a brown solid. $R_f=0.33$ (CS_2/toluene 9:1); ^1H NMR (500 MHz, $CDCl_3$): $\delta=7.98$ (br s, 2 H, ArH), 7.56 (d, $J=8.6$ Hz, 2 H, ArH), 7.49 (br d, $J=8.2$ Hz, 2 H, ArH), 7.13 (app. t, $J=2.2$ Hz, 2 H, pyrrole α-H), 7.03 (d, $J=8.6$ Hz, 2 H, ArH), 6.34 (app. t, $J=2.2$ Hz, 2 H, pyrrole β-H), 5.19 (s, 1 H, pyrrolidine α-CH), 4.86 (d, $J=9.5$ Hz, 1 H, pyrrolidine α-CH_2), 4.51 (d, $J=13.2$ Hz, 1 H, NCH_2Ar), 4.18 (d, $J=9.5$ Hz, 1 H, pyrrolidine α-CH_2), 4.00 (t, $J=6.5$ Hz, 2 H, $OCH_2CH_2CH_3$), 3.68 (d, $J=13.2$ Hz, 1 H, NCH_2Ar), 1.86 (qt, $J=7.4$, 6.5 Hz, 2 H, $OCH_2CH_2CH_3$), 1.08 ppm (t, $J=7.4$ Hz, 3 H, $OCH_2CH_2CH_3$); ^{13}C NMR (125 MHz, $CDCl_3$): $\delta=158.9$, 156.5, 154.2, 153.4, 153.4, 147.5, 147.5, 146.8, 146.6, 146.4, 146.4, 146.4, 146.3, 146.3, 146.3, 146.2, 146.1, 146.1, 145.9, 145.7, 145.5, 145.37, 145.4, 145.4, 145.4, 145.3, 144.9, 144.8, 144.6, 144.5, 143.3, 143.1, 142.8, 142.7, 142.7, 142.7, 142.5, 142.4, 142.3, 142.3, 142.2, 142.2, 142.2, 142.1, 142.0, 142.0, 141.8, 141.7, 140.8, 140.3, 140.3, 140.1, 139.7, 137.1, 136.6, 136.1, 135.8, 134.5, 130.8 (br), 130.3, 129.4, 120.5 (br), 119.2, 114.8, 110.8, 80.7, 76.8, 69.7, 68.7, 66.6, 56.2, 22.8, 10.8 ppm. IR (ATR): $\tilde{\nu}=2917$, 2777, 2326, 1607, 1518, 1324, 1225, 1168, 1065, 1015 cm^{-1}; MS (MALDI −ve): *m/z*: 1052 $[M]^-$; elemental analysis calcd (%) for $C_{82}H_{24}N_2O$: C 93.52, H 2.30, N: 2.66; found: C 93.58, H 2.26, N 2.59.

Compound 13: A mixture consisting of C_{60} (197 mg, 0.273 mmol), **11** (27 mg, 0.158 mmol), and amino acid **5** (227 mg, 0.774 mmol) in degassed toluene (50 mL) was heated under reflux for 12 h. The vessel was allowed to cool to RT and toluene was removed under reduced pressure to give a brown crude residue, which was subjected to flash column chromatography (SiO_2, gradient elution with 1–20 % toluene/CS_2) to provide **13** (69 mg, 39 %) as a brown solid. $R_f=0.80$ (CS_2/toluene 4/1); ^1H NMR (500 MHz, $CDCl_3$): $\delta=7.98$ (br s, 2 H, ArH), 7.50 (br d, $J=8.2$ Hz, 2 H, ArH), 7.25 (s, 2 H, ArH), 7.13 (app. t, $J=2.2$ Hz, 2 H, pyrrole α-H), 6.34 (app. t, $J=2.2$ Hz, 2 H, pyrrole β-H), 5.18 (s, 1 H, pyrrolidine α-CH), 4.88 (d, $J=9.5$ Hz, 1 H, pyrrolidine α-CH_2), 4.45 (d, $J=13.1$ Hz, 1 H, NCH_2Ar), 4.17 (d, $J=9.5$ Hz, 1 H, pyrrolidine α-CH_2), 3.83 (t, $J=6.6$ Hz, 2 H, OCH_2), 3.60 (d, $J=13.1$ Hz, 1 H, NCH_2Ar), 2.39 (s, 6 H, 2 × $ArCH_3$), 1.88–1.82 (m, 2 H, CH_2), 1.57–1.51 (m, 2 H, CH_2), 1.40–1.37 (m, 4 H, 2 × CH_2), 0.93 ppm (t, $J=7.1$ Hz, 3 H, CH_2CH_3); ^{13}C NMR (125 MHz, $CDCl_3$): $\delta=156.5$, 155.8, 154.2, 153.5, 153.4, 147.5, 146.8, 146.6, 146.4, 146.4, 146.4, 146.3, 146.3, 146.3, 146.1, 146.1, 145.9, 145.7, 145.7, 145.5, 145.4, 145.4, 145.4, 145.3, 144.9, 144.8, 144.8, 144.6, 144.5, 143.3, 143.1, 142.8, 142.7, 142.7, 142.7, 142.5, 142.4, 142.3, 142.3, 142.3, 142.2, 142.2, 142.2, 142.1, 142.1, 142.0, 142.0, 141.8, 141.7, 140.8, 140.3, 140.2, 140.1, 139.7, 137.1, 136.6, 136.1, 135.8, 134.5, 132.4, 131.3, 130.8 (br), 129.6, 120.4 (br), 119.2, 110.8, 80.9, 76.8, 72.6, 68.8, 66.8, 56.6, 31.9, 30.6, 26.0, 22.8, 16.7, 14.3 ppm; MS (MALDI −ve) *m/z* 1122 $[M]^-$; elemental analysis calcd (%) for $C_{87}H_{34}N_2O$: C 93.03, H 3.05, N 2.50; found: C 92.97, H 3.14, N 2.50.

***N′*-Formylphenyl-2-{4,5-bis(1-propylthio)-1,3-dithiol-2-yliden}-[1,3]dithiolo[4,5-*c*]pyrrole (14)**: (±)-*trans*-1,2-Diaminocyclohexane (0.04 mL, 0.33 mmol) was added to a microwave tube containing a degassed suspension of MPTTF **3** (40.8 mg, 0.104 mmol), 4-iodobenzaldehyde (118 mg, 0.51 mmol), CuI (39 mg, 0.204 mmol), and K_3PO_4 (83.5 mg, 0.393 mmol) in THF (5 mL) and the contents of the vessel heated for 3 h at 100 °C. The vessel was cooled to RT, after which the mixture was partitioned with CH_2Cl_2 and water and the phases separated. The organic phase was washed with H_2O (4 × 20 mL) and dried over Na_2SO_4, after which the solvent was removed in vacuo. The crude residue was subjected to flash column chromatography (SiO_2, CH_2Cl_2/petroleum ether 7/3) to give pure compound **14** as a crystalline yellow solid (42.5 mg, 82 %). $R_f=0.35$ (CH_2Cl_2/petroleum ether 1/1); m.p. = 208–209 °C; ^1H NMR (500 MHz, CD_2Cl_2): $\delta=9.97$ (s, 1 H, CHO), 7.94 (d, $J=8.6$ Hz, 2 H, ArH), 7.48 (d, $J=8.6$ Hz, 2 H, ArH), 7.05 (s, 2 H, pyrrole α-H), 2.82 (t, $J=7.2$ Hz, 4 H, 2 × $SCH_2CH_2CH_3$), 1.67 (sextet, $J=7.2$ Hz, 4 H, 2 × $SCH_2CH_2CH_3$), 1.01 ppm (t, $J=7.2$ Hz, 6 H, 2 × $SCH_2CH_2CH_3$); ^{13}C NMR (125 MHz, CD_2Cl_2): $\delta=191.0$, 144.6, 134.2, 132.0, 128.2, 124.6, 119.6, 118.4, 113.2, 111.0, 38.8, 23.7, 13.5 ppm; IR (ATR): $\tilde{\nu}=3358$, 3138, 2960, 2928, 2869, 2808, 2735, 1696, 1599, 1585, 1380, 1170, 1035 cm^{-1}; MS (MALDI +ve): *m/z* 496 $[M+H]^+$; elemental analysis calcd (%) for $C_{21}H_{21}S_6NO$: C 50.87, H 4.27, N 2.83; found: C 50.92, H 4.34, N 2.78.

Compound 15: A mixture of C_{60} (133 mg, 0.185 mmol), **14** (43 mg, 0.087 mol), and amino acid **4** (109 mg, 0.488 mmol) in degassed toluene (50 mL) was heated under reflux for 12 h. The vessel was allowed to reach RT and the solvent was evaporated by rotary evaporation to give a brown residue, which was purified by flash column chromatography (SiO_2, gradient elution with 1–10 % toluene/CS_2) to yield compound **15** (69 mg, 58 %) as a brown solid. $R_f=0.85$ (CS_2/toluene 9/1); ^1H NMR (500 MHz, CS_2/C_6D_6 1/1): $\delta=7.98$ (br s, 2 H, ArH), 7.41 (d, $J=8.5$ Hz, 2 H, ArH), 7.07 (br d, $J=7.2$ Hz, 2 H, ArH), 6.88 (d, $J=8.5$ Hz, 2 H, ArH), 6.43 (s, 2 H, pyrrole α-H), 5.03 (s, 1 H, pyrrolidine α-CH), 4.75 (d, $J=9.5$ Hz, 1 H, pyrrolidine α-CH_2), 4.36 (d, $J=13.0$ Hz, 1 H, NCH_2), 4.01 (d, $J=9.5$ Hz, 1 H, pyrrolidine α-CH_2), 3.77 (t, $J=6.4$ Hz, 2 H, $OCH_2CH_2CH_3$), 3.47 (d, $J=13.0$ Hz, 1 H, NCH_2), 2.61 (t, $J=7.2$ Hz, 4 H, 2 × $SCH_2CH_2CH_3$), 1.71 (sextet, $J=7.0$ Hz, 2 H, $OCH_2CH_2CH_3$), 1.52 (sextet, $J=7.2$ Hz, 4 H, 2 × $SCH_2CH_2CH_3$), 0.97 (t, $J=7.4$ Hz, 3 H, $OCH_2CH_2CH_3$), 0.88 ppm (t, $J=7.3$ Hz, 6 H, 2 × $SCH_2CH_2CH_3$); ^{13}C NMR (125 MHz, CS_2/C_6D_6 1/1): $\delta=159.3$, 156.5, 154.1, 153.4, 153.3, 147.6, 147.6, 146.9, 146.7, 146.6, 146.6, 146.5, 146.5, 146.4, 146.3, 146.0, 145.9, 145.8, 145.7, 145.6, 145.6, 145.5, 145.1, 144.9, 144.8, 144.7, 143.6, 143.4, 143.1, 143.0, 143.0, 142.9, 142.7, 142.6, 142.5, 142.5, 142.4, 142.4, 142.4, 142.3, 142.2, 142.2, 142.0, 142.0, 140.6, 140.6, 140.4, 140.3, 140.0, 137.4, 136.7, 136.4, 136.0, 134.8, 131.0 (br), 130.3, 129.2, 128.4, 123.6, 119.9 (br), 115.1, 110.7, 80.9, 76.9, 69.6, 68.8, 66.8, 56.5, 38.7, 23.8, 23.4, 13.7, 11.2 ppm; MS (MALDI −ve) *m/z* 1376 $[M]^-$; IR (ATR): $\tilde{\nu}=2954$, 2917, 2864, 2780, 2361, 2326, 1606, 1508, 1292, 1226, 1169 cm^{-1}; elemental analysis calcd (%) for $C_{92}H_{36}S_6N_2O$: C 80.23, H 2.64, N 2.04; found: C 80.31, H 2.61, N 2.10.

Compound 16: A degassed solution of C_{60} (131 mg, 0.182 mmol), **14** (42 mg, 0.0847 mmol), and amino acid **5** (125 mg, 0.426 mmol) in toluene (50 mL) was heated under reflux for 12 h. The vessel was cooled to RT and the solvent evaporated under reduced pressure to give a brown residue that was purified by flash column chromatography (SiO_2, gradient elution with 1–20% toluene/CS_2) to afford **16** (73 mg, 60%) as a brown solid. $R_f = 0.80$ (CS_2/toluene 4/1); ^{1}H NMR (500 MHz, CS_2/C_6D_6 1/1): $\delta = 7.82$ (br s, 2H, ArH), 7.20 (s, 2H), 7.06 (br d, $J = 6.4$ Hz, 2H, ArH), 6.37 (s, 2H, pyrrole α-H), 5.04 (s, 1H, pyrrolidine α-CH), 4.80 (d, $J = 9.5$ Hz, 1H, pyrrolidine α-CH_2), 4.35 (d, $J = 12.9$ Hz, 1H, NCH_2Ar), 4.03 (d, $J = 9.5$ Hz, 1H, pyrrolidine α-CH_2), 3.69 (t, $J = 6.5$ Hz, 2H, OCH_2), 3.42 (d, $J = 12.9$ Hz, 1H, NCH_2Ar), 2.60 (t, $J = 7.1$ Hz, 4H, $2\times SCH_2CH_2CH_3$), 2.32 (s, 6H, $2\times ArCH_3$), 1.77–1.71 (m, 2H), 1.55–1–44 (m, 6H), 1.32–1.29 (m, 4H, $2\times CH_2$), 0.90 (t, $J = 7.0$ Hz, 3H), 0.87 ppm (t, $J = 7.3$ Hz, 6H, $2\times SCH_2CH_2CH_3$); ^{13}C NMR (125 MHz, CS_2/C_6D_6 1/1): $\delta = 156.5$, 156.3, 154.2, 153.4, 153.3, 147.6, 147.6, 146.9, 146.7, 146.7, 146.6, 146.6, 146.5, 146.5, 146.4, 146.3, 146.3, 146.0, 146.0, 145.9, 145.8, 145.8, 145.7, 145.7, 145.6, 145.6, 145.5, 145.1, 144.9, 144.5, 144.8, 144.7, 143.6, 143.4, 143.1, 143.0, 143.0, 142.9, 142.7, 142.6, 142.5, 142.45, 142.4, 142.4, 142.4, 142.3, 142.2, 142.2, 142.0, 142.0, 140.6, 140.6, 140.4, 140.3, 140.3, 140.0, 137.4, 136.7, 136.4, 136.0, 134.9, 132.5, 131.5, 130.9 (br), 129.9, 128.4, 123.6, 119.9 (br), 119.6, 112.4, 110.7, 81.2, 77.0, 72.5, 68.9, 67.0, 57.1, 38.7, 32.4, 31.1, 26.6, 23.8, 23.5, 17.0, 14.7, 13.6 ppm; MS (MALDI −ve): *m/z* 1446 $[M]^-$; IR (ATR): $\tilde{\nu} = 2951$, 2914, 2850, 2362, 2342, 1736, 1607, 1514 1374, 1306, 1214, 1176, 1143, 1038 cm^{-1}; elemental analysis calcd (%) for $C_{97}H_{46}N_2OS_6$: C 80.49, H 3.21, N 1.94; found: C 80.31, H 3.22, N 2.03.

Bis-{*N*′(4-(formylphenyl)pyrrolo[3,4-*d*])}tetrathiafulvalene (17): (±)-*trans*-1,2-Diaminocyclohexane (0.05 mL, 0.42 mmol) was added to a microwave tube containing a degassed suspension of **2** (29.8 mg, 0.105 mmol), 4-iodobenzaldehyde (121 mg, 0.52 mmol), CuI (40 mg, 0.21 mmol), and K_3PO_4 (77.7 mg, 0.34 mmol) in THF (5 mL). The reaction mixture was heated conventionally for 22 h at 105 °C, cooled to RT, and filtered. The red-brown solid was washed with the following sequence of solvents, whereby the precipitate was suspended in the solvent, sonicated, and centrifuged, and finally the solvent was decanted from the solid: water (2×5 mL), H_2O/CH_3CN (1/1, 2×5 mL), MeCN (2×5 mL), MeOH (2×5 mL), EtOAc (2×5 mL), THF/Et_2O (1/1, 2×5 mL), Et_2O (2×5 mL), and pentanes (2×5 mL) to give compound **17** (24 mg, 45%) as a brick orange solid. IR (ATR): $\tilde{\nu} = 3140$, 2927, 2846, 1687, 1598, 1515, 1382, 1305, 1167, 1111, 1024, 822 cm^{-1}; MS (MALDI +ve): *m/z* 490 $[M]^+$; elemental analysis calcd (%) for $C_{24}H_{14}S_4N_2O_2$: C 58.75, H 2.88, N 5.71; found: C 58.77; H 2.90; N 5.63.

Compound 18: Compounds **4** (123 mg, 0.551 mmol) and **17** (18.3 mg, 0.038 mmol) were added to a degassed sonicated solution of C_{60} (116 mg, 0.160 mmol) in *o*-DCB (42 mL) and the mixture was heated at 150 °C for 18 h. The vessel was allowed to cool to ambient temperature and the residue purified by flash column chromatography (SiO_2, gradient elution with 2–25% toluene/CS_2) to give **18** (18 mg, 21%) as a brown solid. $R_f = 0.48$ (CS_2/toluene 17/3); ^{1}H NMR (500 MHz, CS_2/C_6D_6 1/1): $\delta = 7.79$ (br s, 4H, ArH), 7.40 (d, $J = 8.6$ Hz, 4H, ArH), 7.09 (br d, 4H, $J = 8.3$ Hz, ArH), 6.87 (d, $J = 8.6$ Hz, 4H, ArH), 6.45 (s, 4H, pyrrole α-H), 5.03 (s, 2H, pyrrolidine α-CH), 4.74 (d, $J = 9.5$ Hz, 2H, pyrrolidine α-CH_2), 4.36 (d, $J = 13.1$ Hz, 2H, NCH_2Ar), 4.01 (d, $J = 9.5$ Hz, 2H, pyrrolidine α-CH_2), 3.77 (t, 4H, $J = 6.4$ Hz, $2\times OCH_2CH_2CH_3$), 3.47 (d, $J = 13.1$ Hz, 2H, NCH_2Ar), 1.71 (sextet, $J = 7.4$ Hz, 4H, $2\times OCH_2CH_2CH_3$), 0.97 ppm (t, $J = 7.4$ Hz, 6H, $2\times OCH_2CH_2CH_3$); ^{13}C NMR (125 MHz, CS_2/C_6D_6 1/1): $\delta = 159.2$, 156.5, 154.1, 153.4 153.3, 147.6, 147.6, 146.9, 146.7, 146.6, 146.6, 146.5, 146.5, 146.4, 146.4, 146.3, 146.0, 145.9, 145.9, 145.8, 145.8, 145.7, 145.6, 145.5, 145.5, 145.1, 144.9, 144.8, 144.7, 143.5, 143.4, 143.1, 143.0, 142.9, 142.9, 142.7, 142.6, 142.5, 142.5, 142.4, 142.4, 142.3, 142.2, 142.0, 141.9, 140.6, 140.6, 140.4, 140.3, 140.0, 137.3, 136.7, 136.4, 136.0, 134.7, 130.9 (br), 130.3, 129.2, 128.4, 123.6, 120.0 (br), 115.1, 110.6, 80.9, 76.9, 69.6, 68.8, 66.9, 56.5, 23.5, 11.2 ppm; MS (MALDI −ve): *m/z* 2252 $[M]^-$; elemental analysis calcd (%) for $C_{166}H_{44}N_4O_2S_4$: C 88.45, H 1.97, N 2.49; found: C 88.57, H 2.11, N 2.42.

Compound 19: A thoroughly sonicated and degassed mixture of C_{60} (31.1 mg, 41 µmol), **17** (5.6 mg, 11.4 µmol), amino acid **5** (37.5 mg, 0.127 mmol), and Proton Sponge (5.8 mg, 27.1 µmol) in *o*-DCB (40 mL) was heated at 150 °C for 22 h. The vessel was allowed to cool to RT and the solvent was evaporated under high vacuum to give a brown residue, which was subjected to purification by flash column chromatography (SiO_2, gradient elution with 2–25% toluene/CS_2) to provide **19** (6.6 mg, 24%) as a brown solid; $R_f = 0.40$ (CS_2/toluene 4/1); ^{1}H NMR (500 MHz, CS_2/C_6D_6 1/1): $\delta = 7.81$ (br s, 4H, ArH), 7.13 (s, 4H, ArH), 6.51 (s, 4H, pyrrole α-H), 5.03 (s, 2H, 2×pyrrolidine α-CH), 4.77 (d, $J = 9.5$ Hz, 2H, pyrrolidine α-CH_2), 4.32 (d, $J = 12.9$ Hz, 2H, NCH_2Ar), 4.03 (d, $J = 9.5$ Hz, 2H, pyrrolidine α-CH_2), 3.67 (t, $J = 6.5$ Hz, 4H, $2\times OCH_2$), 3.41 (d, $J = 12.9$ Hz, 2H, NCH_2Ar), 2.28 (s, 12H, $4\times ArCH_3$), 1.75–1.69 (m, 4H, $2\times CH_2$), 1.49–1.43 (m, 4H, $2\times CH_2$), 1.32–1.25 (m, 8H, $4\times CH_2$), 0.89 ppm (t, $J = 6.9$ Hz, 6H, $2\times CH_3$), one aromatic signal not observable either due to broadening or it being hidden under the benzene resonances; ^{13}C NMR (125 MHz, CS_2/C_6D_6 1/1) $\delta = 156.4$, 156.2, 154.1, 153.4, 153.2, 147.6, 147.6, 146.8, 146.6, 146.5, 146.5, 146.4, 146.4, 146.3, 146.2, 146.2, 146.0, 145.9, 145.9, 145.7, 145.7, 145.6, 145.6, 145.5, 145.5, 145.4, 145.0, 144.9, 144.7, 144.6, 143.5, 143.3, 143.0, 143.0, 142.9, 142.6, 142.5, 142.4, 142.4, 142.3, 142.3, 142.2, 142.1, 141.9, 140.6, 140.5, 140.3, 139.9, 137.3, 136.7, 136.3, 135.9, 134.8, 132.4, 131.4, 130.9 (br), 129.8, 128.4, 123.7, 121.2, 119.9 (br), 110.6, 81.2, 76.9, 72.4, 68.8, 67.0, 57.1, 32.5, 31.2, 26.6, 23.6, 17.0, 14.8 ppm; MS (MALDI −ve): *m/z* 2392 $[M^-]$; elemental analysis calcd (%) for $C_{176}H_{64}N_4O_2S_4$: C 88.28, H 2.70, N 2.34; found: C 88.32, H 2.81, N 2.19.

Acknowledgements

This work was supported by the European Commission (EC) FP7 Initial Training Networks (ITN) “FUNMOLS” Project No. 212942 and “MOLESCO” Project No. 606728, the University of Southern Denmark, the University of Copenhagen, the Danish Council for Independent Research-Natural Sciences (#10-082088 and 11-106744), and the Danish-Chinese Center for Molecular Nanoelectronics funded by the Danish National Research Foundation.

Keywords: cycloaddition · donor–acceptor systems · fullerenes · monolayers · tetrathiafulvalenes

[1] a) Y. Luo, C. P. Collier, J. O. Jeppesen, K. A. Nielsen, E. Delonno, G. Ho, J. Perkins, H.-R. Tseng, T. Yamamoto, J. F. Stoddart, J. R. Heath, *ChemPhysChem* **2002**, *3*, 519–525; b) D. R. Stewart, D. A. A. Ohlberg, P. A. Beck, Y. Chen, R. S. Williams, J. O. Jeppesen, K. A. Nielsen, J. F. Stoddart, *Nano Lett.* **2004**, *4*, 133–136; c) G. Ho, J. R. Heath, M. Kondratenko, D. F. Perepichka, K. Arseneault, M. Pézolet, M. R. Bryce, *Chem. Eur. J.* **2005**, *11*, 2914–2922; d) E. Leary, S. J. Higgins, H. van Zalinge, W. Haiss, R. J. Nichols, S. Nygaard, J. O. Jeppesen, J. Ulstrup, *J. Am. Chem. Soc.* **2008**, *130*, 12204–12205; e) J. Liao, J. S. Agustsson, S. Wu, C. Schönenberger, M. Calame, Y. Leroux, M. Mayor, O. Jeannin, Y.-F. Ran, S.-X. Liu, S. Decurtins, *Nano Lett.* **2010**, *10*, 759–764; f) A. Coskun, J. M. Spruell, G. Barin, Y. Y. Botros, J. F. Stoddart, *Chem. Soc. Rev.* **2012**, *41*, 4827–4859; g) J. Fock, M. Leijnse, K. Jennum, A. S. Zyazin, J. Paaske, P. Hedegård, M. B. Nielsen, H. S. J. van der Zant, *Phys. Rev. B* **2012**, *86*, 235–403; h) C. R. Parker, Z. Wei, C. A. Rodríguez, K. Jennum, T. Li, M. Santella, N. Bovet, G. Yhao, W.

Hu, H. S. J. van der Zant, M. Vanin, G. C. Solomon, B. W. Laursen, K. Nørgaard, M. B. Nielsen, *Adv. Mater.* **2013**, *25*, 405 – 409.

[2] Thiolates are widely exploited as anchoring groups; for a review, see K. Nørgaard, M. B. Nielsen, T. Bjørnholm, in *Functional Organic Materials* (Eds.: T. J. J. Müller, U. H. F. Bunz), Wiley-VCH, Weinheim **2007**, p. 353 – 392.

[3] a) C. A. Martin, D. Ding, J. K. Sørensen, T. Bjørnholm, J. M. van Ruitenbeek, H. S. J. van der Zant, *J. Am. Chem. Soc.* **2008**, *130*, 13198 – 13199; b) E. Leary, M. T. González, C. van der Pol, M. R. Bryce, S. Filippone, N. Martín, G. Rubio-Bollinger, N. Agraït, *Nano Lett.* **2011**, *11*, 2236 – 2241.

[4] a) M. Maggini, G. Scorrano, M. Prato, *J. Am. Chem. Soc.* **1993**, *115*, 9798 – 9799; b) M. Maggini, G. Scorrano, A. Bianco, C. Toniolo, R. P. Sijbesma, F. Wudl, M. Prato, *J. Chem. Soc. Chem. Commun.* **1994**, 305 – 306; c) M. Prato, M. Maggini, C. Giacometti, G. Scorrano, G. Sandonà, G. Farnia, *Tetrahedron* **1996**, *52*, 5221 – 5234; d) M. Prato, M. Maggini, *Acc. Chem. Res.* **1998**, *31*, 519 – 526; e) N. Tagmatarchis, M. Prato, *Synlett* **2003**, 768 – 779.

[5] a) C. van der Pol, M. R. Bryce, M. Wielopolski, C. Atienza-Castellanos, D. M. Guldi, S. Filippone, N. Martín, *J. Org. Chem.* **2007**, *72*, 6662 – 6671; b) J. K. Sørensen, J. Fock, A. H. Pedersen, A. B. Petersen, K. Jennum, K. Bechgaard, K. Kilså, V. Geskin, J. Cornil, T. Bjørnholm, M. B. Nielsen, *J. Org. Chem.* **2011**, *76*, 245 – 263.

[6] a) D. Kreher, M. Cariou, S.-G. Liu, E. Levillain, J. Veciana, C. Rovira, A. Gorgues, P. Hudhomme, *J. Mater. Chem.* **2002**, *12*, 2137 – 2159; b) D. Kreher, P. Hudhomme, A. Gorgues, H. Luo, Y. Araki, O. Ito, *Phys. Chem. Chem. Phys.* **2003**, *5*, 4583 – 4592.

[7] J. L. Segura, E. M. Priego, N. Martín, C. Luo, D. M. Guldi, *Org. Lett.* **2000**, *2*, 4021 – 4024.

[8] N. Martín, L. Sánchez, M. Á. Herranz, B. Illescas, D. M. Guldi, *Acc. Chem. Res.* **2007**, *40*, 1015 – 1024.

[9] For other dyads and triads, see M. Bendikov, F. Wudl, D. F. Perepichka, *Chem. Rev.* **2004**, *104*, 4891 – 4945.

[10] a) J. O. Jeppesen, K. Takimiya, F. Jensen, J. Becher, *Org. Lett.* **1999**, *1*, 1291 – 1294; b) J. O. Jeppesen, K. Takimiya, F. Jensen, T. Brimert, K. Nielsen, N. Thorup, J. Becher, *J. Org. Chem.* **2000**, *65*, 5794 – 5805.

[11] a) J. O. Jeppesen, J. Becher, *Eur. J. Org. Chem.* **2003**, 3245 – 3266; b) J. A. Hansen, J. Becher, J. O. Jeppesen, E. Levillain, M. B. Nielsen, B. M. Petersen, J. C. Petersen, Y. Şahin, *J. Mater. Chem.* **2004**, *14*, 179 – 184; c) K. A. Nielsen, E. Levillain, V. M. Lynch, J. L. Sessler, J. O. Jeppesen, *Chem. Eur. J.* **2009**, *15*, 506 – 516.

[12] a) G. W. Gray, B. Jones, *J. Chem. Soc.* **1954**, 1467 – 1470; b) M. Santella, V. Mazzanti, M. Jevric, C. R. Parker, S. L. Broman, A. D. Bond, M. B. Nielsen, *J. Org. Chem.* **2012**, *77*, 8922 – 8932.

[13] Reference data for compound **7**: P. Hindmarsh, M. Hird, P. Styring, J. W. Goodby, *J. Mater. Chem.* **1993**, *3*, 1117 – 1128.

[14] a) J. F. Hartwig, *Acc. Chem. Res.* **1998**, *31*, 852 – 860; b) J. P. Wolfe, S. Wagaw, J.-F. Marcoux, S. L. Buchwald, *Acc. Chem. Res.* **1998**, *31*, 805 – 818; c) J. F. Hartwig, *Angew. Chem.* **1998**, *110*, 2154 – 2177; *Angew. Chem. Int. Ed.* **1998**, *37*, 2046 – 2067; d) A. Klapars, J. C. Antilla, X. Huang, S. L. Buchwald, *J. Am. Chem. Soc.* **2001**, *123*, 7727 – 7729; e) J. C. Antilla, J. M. Baskin, T. E. Barder, S. L. Buchwald, *J. Org. Chem.* **2004**, *69*, 5578 – 5587; f) C. Fischer, B. Koenig, *Beilstein J. Org. Chem.* **2011**, *7*, 59 – 74.

[15] a) H. Li, C. Lambert, *Chem. Eur. J.* **2006**, *12*, 1144 – 1155; b) Y. Salinas, M. V. Solano, R. E. Sørensen, K. R. Larsen, J. Lycoops, J. O. Jeppesen, R. Martínez-Máñez, F. Sancenón, M. D. Marcos, P. Amorós, C. Guillem, *Chem. Eur. J.* **2014**, *20*, 855 – 866.

[16] Compound **17** was used as the limiting reagent for the formation of triads **18** and **19**; therefore, the yields calculated for the byproducts **20 a**–**b** and **21 a**–**b** are based on the amount of **17**.

[17] a) F. Gerson, E. Haselbach, G. Plattner, *Chem. Phys. Lett.* **1971**, *12*, 316 – 319; b) A. Szemik-Hojniak, W. Rettig, I. Deperasinska, *Chem. Phys. Lett.* **2001**, *343*, 404 – 412.

[18] Even with the use of Proton Sponge, substantial amounts of byproducts **20 a**–**b** and **21 a**–**b** were formed.

[19] a) N. Martín, M. Altable, S. Filippone, A. Martín-Domenech, L. Echegoyen, C. M. Cardona, *Angew. Chem.* **2006**, *118*, 116 – 120; *Angew. Chem. Int. Ed.* **2006**, *45*, 110 – 114; b) J. L. Delgado, F. Oswald, F. Cardinali, F. Langa, N. Martín, *J. Org. Chem.* **2008**, *73*, 3184 – 3188.

[20] B. Ma, Y.-P. Sun, *J. Chem. Soc. Perkin Trans. 2* **1996**, 2157 – 2162.

[21] a) C. M. Yip, M. D. Ward, *Langmuir* **1994**, *10*, 549 – 556; b) R. Yuge, A. Miyazaki, T. Enoki, K. Tamada, F. Nakamura, M. Hara, *J. Phys. Chem. B* **2002**, *106*, 6894 – 6901; c) E. J. Pacsial, D. Alexander, R. J. Alvarado, M. Tomasulo, F. M. Raymo, *J. Phys. Chem. B* **2004**, *108*, 19307 – 19313; d) Y. Yokota, A. Miyazaki, K. Fukui, T. Enoki, K. Tamada, M. Hara, *J. Phys. Chem. B* **2006**, *110*, 20401 – 20408; e) P.-Y. Blanchard, O. Aévêque, S. Boisard, C. Gautier, A. El-Ghayoury, F. Le Derf, T. Breton, E. Levillain, *Phys. Chem. Chem. Phys.* **2011**, *13*, 2118 – 2120.

[22] a) E. Gomar-Nadal, G. K. Ramachandran, F. Chen, T. Burgin, C. Rovira, D. B. Amabilino, S. M. Lindsay, *J. Phys. Chem. B* **2004**, *108*, 7213 – 7218; b) L. R. Ditzler, C. Karunatilaka, V. R. Donuru, H. Y. Liu, A. V. Tivanski, *J. Phys. Chem. C* **2010**, *114*, 4429 – 4435.

Received: March 15, 2014